

Results and Discussion

We first investigated the spatially directed formation of QDs in silk protein-expressing *E. coli* cells treated with 1 mM CdCl₂ and Na₂SeO₃. The cells harboring empty vector were similarly excited at 405 nm, and emitted background level of fluorescence serving as a control. Scale bar: 2.5 μm. The fluorescence emission spectra of the control and silk protein-expressing cells at 350 nm excitation. Data in c are presented as mean ± s.d. of n = 3 samples. Statistical significance was determined using one-way analysis of variance (ANOVA) for P values (*P < 0.05; **P < 0.01; ***P < 0.001).

The results showed that the spatially directed formation of QDs in silk protein-expressing *E. coli* cells treated with 1 mM CdCl₂ and Na₂SeO₃ was significantly higher than that of the control cells. The fluorescence emission spectra of the control and silk protein-expressing cells at 350 nm excitation. Data in c are presented as mean ± s.d. of n = 3 samples. Statistical significance was determined using one-way analysis of variance (ANOVA) for P values (*P < 0.05; **P < 0.01; ***P < 0.001).

aggregates [21,22]. The fluorescence emission spectra of the control and silk protein-expressing cells at 350 nm excitation. Data in c are presented as mean ± s.d. of n = 3 samples. Statistical significance was determined using one-way analysis of variance (ANOVA) for P values (*P < 0.05; **P < 0.01; ***P < 0.001).

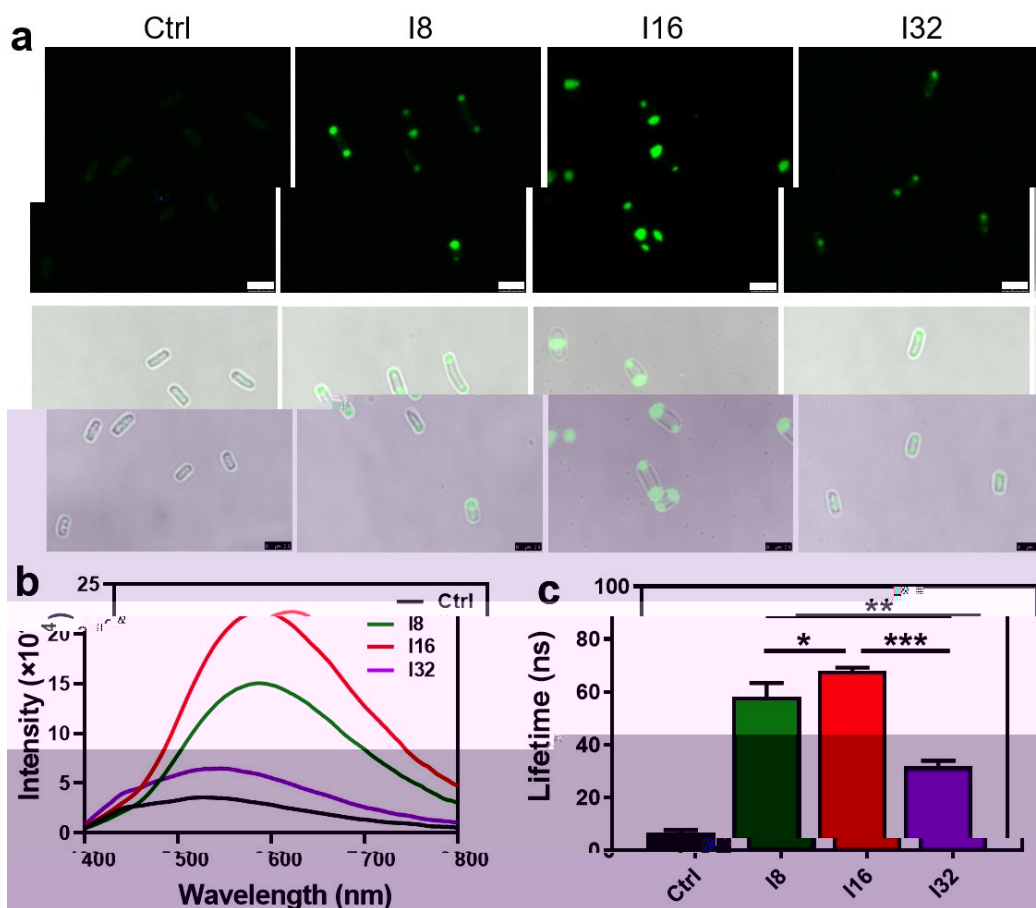


Figure 1. Spatially directed formation of QDs in silk protein-expressing *E. coli* cells. a) Fluorescence microscopy (upper) and merged bright-field and fluorescent images (lower) of the silk protein-expressing cells treated with 1 mM CdCl₂ and Na₂SeO₃. The cells harboring empty vector were similarly excited at 405 nm, and emitted background level of fluorescence serving as a control. Scale bar: 2.5 μm. b) Fluorescence emission spectra of the control and silk protein-expressing cells at 350 nm excitation. c) Fluorescence lifetime of the biogenic QDs from the respective *E. coli* cells. Data in c are presented as mean ± s.d. of n = 3 samples. Statistical significance was determined using one-way analysis of variance (ANOVA) for P values (*P < 0.05; **P < 0.01; ***P < 0.001).

estates (Figure S6). Ultrastructural analysis of the weaverite crystals revealed a width of 50 nm (Figure S6b) which was in accordance with the average width of the weaverite crystals (FW_{TM}) from the natural sample (CSe_xS_{1-x})¹¹. The full width at half maximum (FWHM) of the (001) reflection of CSe_xS_{1-x} was about 192 nm, which is in agreement with the value of 140 nm reported by the authors for the natural sample.¹¹ The FWHM of the (001) reflection of the synthesized weaverite crystals was 160 nm, which is in agreement with the value of 166 nm reported by the authors for the natural sample.¹¹ The lattice spacing of the (001) reflection of CSe_xS_{1-x} was 160 nm, which is in agreement with the value of 166 nm reported by the authors for the natural sample.¹¹ The lattice spacing of the (001) reflection of CSe_xS_{1-x} was 160 nm, which is in agreement with the value of 166 nm reported by the authors for the natural sample.¹¹

The weaverite crystals grown from the CSe_xS_{1-x} were characterized by XRD. The XRD patterns of the weaverite crystals grown from the CSe_xS_{1-x} were in good agreement with the pattern of the weaverite crystals grown from the natural sample (Figure S8). The weaverite crystals grown from the CSe_xS_{1-x} were characterized by XRD. The XRD patterns of the weaverite crystals grown from the CSe_xS_{1-x} were in good agreement with the pattern of the weaverite crystals grown from the natural sample (Figure S8). The weaverite crystals grown from the CSe_xS_{1-x} were characterized by XRD. The XRD patterns of the weaverite crystals grown from the CSe_xS_{1-x} were in good agreement with the pattern of the weaverite crystals grown from the natural sample (Figure S8).

For reference, the weaverite crystals grown from the natural sample were characterized by XRD. The XRD patterns of the weaverite crystals grown from the natural sample were in good agreement with the pattern of the weaverite crystals grown from the natural sample (Figure S8). The weaverite crystals grown from the natural sample were characterized by XRD. The XRD patterns of the weaverite crystals grown from the natural sample were in good agreement with the pattern of the weaverite crystals grown from the natural sample (Figure S8).

very effective in the growth of the weaverite crystals. The weaverite crystals grown from the natural sample were characterized by XRD. The XRD patterns of the weaverite crystals grown from the natural sample were in good agreement with the pattern of the weaverite crystals grown from the natural sample (Figure S8). The weaverite crystals grown from the natural sample were characterized by XRD. The XRD patterns of the weaverite crystals grown from the natural sample were in good agreement with the pattern of the weaverite crystals grown from the natural sample (Figure S8).

Further, the weaverite crystals grown from the natural sample were characterized by XRD. The XRD patterns of the weaverite crystals grown from the natural sample were in good agreement with the pattern of the weaverite crystals grown from the natural sample (Figure S8). The weaverite crystals grown from the natural sample were characterized by XRD. The XRD patterns of the weaverite crystals grown from the natural sample were in good agreement with the pattern of the weaverite crystals grown from the natural sample (Figure S8).

The weaverite crystals grown from the natural sample were characterized by XRD. The XRD patterns of the weaverite crystals grown from the natural sample were in good agreement with the pattern of the weaverite crystals grown from the natural sample (Figure S8). The weaverite crystals grown from the natural sample were characterized by XRD. The XRD patterns of the weaverite crystals grown from the natural sample were in good agreement with the pattern of the weaverite crystals grown from the natural sample (Figure S8).

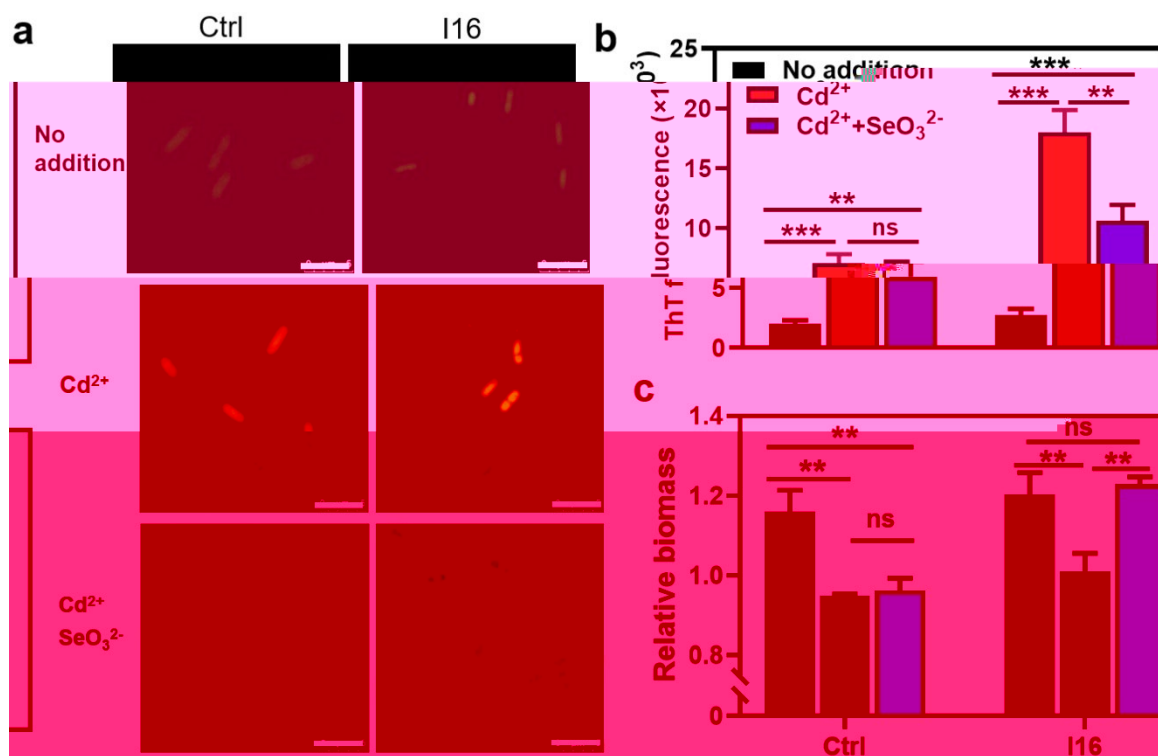
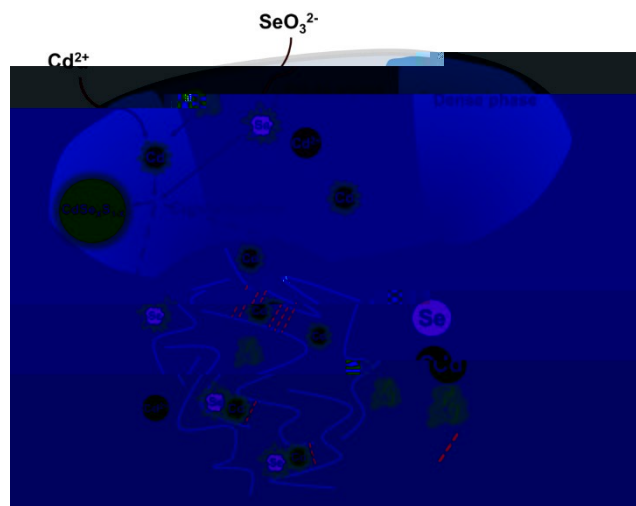


Figure 3. Recovery of bacterial fitness upon QDs biogenesis and co-localization in the synthetic protein condensates. a) Fluorescence microscopy images of the control and I16-expressing *E. coli* cells without and with treatment of Cd²⁺ alone or in combination with SeO₃²⁻. The cells were stained with ThT, a fluorescent probe to detect β -sheet structures, and excited at 458 nm. Scale bars: 5 μ m. b) Fluorescence intensity at 490 nm of the ThT-stained cells. c) Effect of ion treatment on the cell growth. The ratio of cell biomass 4 h after the ion treatment to that just before the treatment was calculated and shown. Data in b and c are presented as mean \pm s.d. of $n = 3$ samples. Statistical significance was determined using one-way ANOVA (ns, not significant with $P > 0.05$; ** $P < 0.01$; *** $P < 0.001$).

...e e ta. fract... a te... r te... e ate were ver...
t reef... ager ta... e ate... ae fte...
(Figure 4) A... e... e... fte... e ate reveal...
t at te S fract... wa a... r... a te... f...
t at fte C... e... t... w... a... a... g... a... e... t...
wit te... r... a... t... r... a... a... t... a...
gr... [33]... t... r... e... t... a... t... e... n... e... t... f... S... e... e... t...
... e... a... t... e... fte... C²⁺... e... n... e... t... a... t... e...
r... t... e... a... t... e... T... e... r... e... t... e... r... t... i... g... g... e... t... a...
... a... e... t... f... o... a... t... e... a... a... q... u... i... r... e... y... t... e... *E. coli*...
... e... t... r... e... f... e... r... e... t... a... l... y... a... C²⁺... a... r... e... o... u... t... f... i... r... o... t... a...
... a... g... r... e... a... g... e... t... w... i... t... t... e... a... r... t... e... e... a... t... e...
... a... e... t... e... a... v... e... r... v... a... t... i... o... n... e... r... e... w... e... r... e... a...
... e... f... r... t... e... a... t... a... y... a... r... e... a... y... t... e... a... a... z... a... t... i... o... n...
f C Se_xS_{1-x}... w... i... t... t... e... a... r... t... e... e... a... t... e... f...
a... t... e... r... *E. coli* (S... e... e... 1) W... e... t... e... a... r... t... e...
e... r... e... i... g... e... w... e... r... e... e... t... t... e... C²⁺... a... r... e... e... a... t... i... o... n...
f... t... e... e... a... v... e... r... v... a... t... i... o... n... a... t... t... e... o... z... o... n... e... f... t... e...
a... t... e... r... a... a... w... e... a... t... a... g... t... t... e... r... e... a... t... a... r...
r... t... e... T... a... a... g... a... t... e... t... e... a... r... t... e... f... r... e...
r... e... t... e... a... r... t... r... o... t... i... o... n... f... a... c... i... l... i... t... a... t... i... o... n... f... o... r... a... r...
t... e... r... a... t... i... o... n... (... a... y... r... g... e... a... g...) f... t... e... a... r... t... e... t...
... e... r... g... S... T... e... a... g... f... C²⁺... a... e... a... e... t... e...
r... t... e... r... a... t... e... a... e... n... o... t... a... o... t... a... g... e... t...
... a... a... t... e... g... i... t... a... t... i... o... n... /... r... e... r... e...
r... e... o... t... a... t... i... o... n... a... r... t... i... c... l... e... f... Se₃²⁻... a... a... g...



Scheme 1. Schematic diagram of spatially directed biosynthesis and localization of CdSe_xS_{1-x} QDs within the subcellular silk protein condensates.

wit... e... r... t... a... t... i... o... n... f... a... c... i... l... i... t... a... t... i... o... n... f... o... r... a... r...
t... e... r... a... t... i... o... n... (... a... y... r... g... e... a... g...) f... t... e... a... r... t... e... t...
... e... r... g... S... T... e... a... g... f... C²⁺... a... e... a... e... t... e...
r... t... e... r... a... t... e... a... e... n... o... t... a... o... t... a... g... e... t...
... a... a... t... e... g... i... t... a... t... i... o... n... /... r... e... r... e...
r... e... o... t... a... t... i... o... n... a... r... t... i... c... l... e... f... Se₃²⁻... a... a... g...

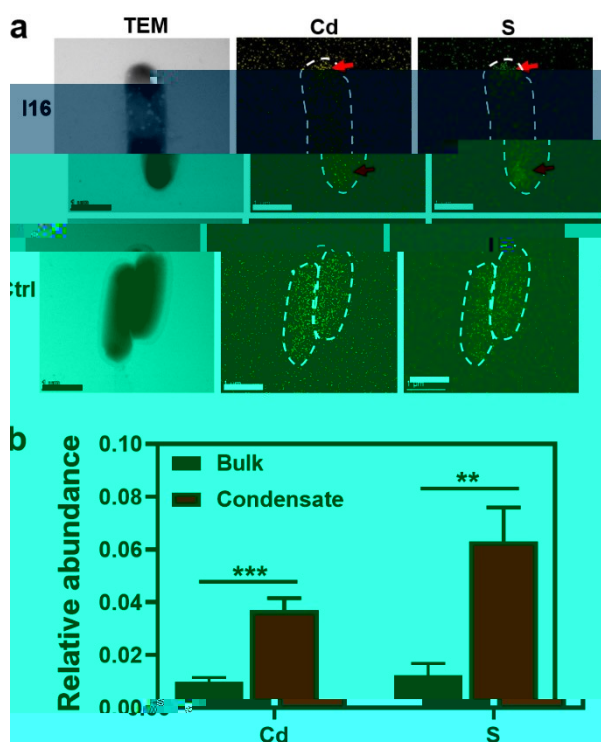


Figure 4. Preferential binding of Cd²⁺ and recruitment of sulfur containing agents within the silk protein I16 condensates. a) TEM images and elemental mapping of the silk protein I16-expressing and control cells treated with Cd²⁺. The red arrows indicate the positions of the silk protein condensates. b) Relative abundance of Cd and S elements within and outside the condensates of the I16-expressing cells with Cd²⁺ treatment. Data in b are presented as mean ± s.d. of n = 3 samples. Statistical significance was determined using one-way ANOVA (**P < 0.01; ***P < 0.001).

the ability of the silk protein condensates to recruit sulfur containing agents within the condensates. The results show that the silk protein condensates have the ability to recruit sulfur containing agents within the condensates.

Conclusion

In this work, we have developed a new strategy for the synthesis of silk protein condensates. The silk protein condensates are able to recruit sulfur containing agents within the condensates. The results show that the silk protein condensates have the ability to recruit sulfur containing agents within the condensates.

advantage. First, the silk protein condensates are able to recruit sulfur containing agents within the condensates. The results show that the silk protein condensates have the ability to recruit sulfur containing agents within the condensates.

Acknowledgements

This work was supported by the National Natural Science Foundation of China (Grant No. 2027FA0909502 and 2027FA0907702) and the Shanghai Science and Technology Commission (Grant No. 2207010732071414 and 22075179) and the Shanghai Science and Technology Commission (Grant No. 21ZJ1432100).

Conflict of Interest

The authors declare no conflict of interest.

Data Availability Statement

The data that support the findings of this study are available in the supplementary material.

Keywords: Biomolecular Condensate · Membraneless Compartment · Quantum Dots · Spider Dragline Silk Protein · Synthetic Biology

- [1] A. Efrati, M. A. A. M. Nat. Nanotechnol. 2018, 13, 278–288.
- [2] J. T. A. A. Nano Lett. 2001, 1, 207–211.
- [3] W. G. Chem. Soc. Rev. 2015, 44, 4792–4834.
- [4] Y. C. S. Y. Nat. Chem. Rev. 2020, 4, 638–656.
- [5] T. W. W. T. Z. C. W. W. G. F. A. Z. G. C. G. Y. G. A. F. Z. G.

